for single-crystal n-type Si-based cells.

The overall efficiency for an a-Si:H cell (Table II) is slightly better than we have typically found for a single-crystal n-type Si-based cell.[16b,17] The output photovoltage is higher, but the quantum yield is lower, for the a-Si:H. The low observed quantum yield is partly due to the fact that the values given are uncorrected for reflection losses of ~30% at 632.8 nm. Another possible loss is the relatively low absorbance of incident 632.8-nm light. The fact that current flows at all is due to the fact that carriers are created throughout the thickness of the film, but not all carriers survive to be collected at the contact and electrolyte. The absorptivity[3] at 632.8 nm is $\sim 10^4$ cm^{-1}, suggesting that a significant number of carriers are generated at a depth of >0.5 μm from the surface. Some photogenerated holes beyond this depth may not arrive at the electrolyte, despite the field driving them toward the electrolyte. Shorter wavelength light is absorbed more strongly such that carriers can be created closer to the surface. However, such will not lead to sufficient carriers deep below the surface to result in a current. Consequently, 454.4- or 514.5-nm light from an Ar ion laser gives lower observed quantum yields than does 632.8-nm light at the same intensity in photons/(cm^2 s). When white light (from an incandescent source, 200-W tungsten lamp) is used to create carriers throughout the material, the observed quantum yield for additional light at 514.5 nm can be determined to be somewhat greater than from additional 632.8-nm light. White light irradiation to give the same current density at E_{redox} as the 632.8-nm light in Figure 5 does not lead to improved fill factors that might be expected for more uniform carrier distribution. The improvements possible with white light alone, or the conversion efficiency from 632.8 or 514.5 nm monochromatic light when the surface is simultaneously illuminated with white light, are not dramatic. Another source of inefficiency may be due to the use of a relatively thick a-Si:H layer. Despite the fact that the material is nearly intrinsic, the low carrier concentration in the 3.9-μm thickness likely means that the field across the material is much stronger near the surface. The point is that the representations in Schemes I–IV showing uniform fields across the photoconductor do not strictly apply to the samples used here. Thinner samples may give improved quantum efficiencies and fill factors since the field could extend across the entire material.

(17) Legg, K. D.; Ellis, A. B.; Bolts, J. M.; Wrighton, M. S. *Proc. Natl. Acad. Sci. U.S.A.* **1977**, *74*, 4116.

Summary

Intrinsic a-Si:H can be used as an electrode in electrochemical cells when ≥1.7-eV light is used to create a significant carrier density throughout the material. For redox couples having $E^{\circ\prime}$ more negative than ~−0.7 V vs. SCE, the electrochemistry occurs at potentials expected for a reversible electrode. For $E^{\circ\prime}$ more positive than −0.7 V vs. SCE, the oxidation of the reduced form of the couple can be effected in an uphill sense using the light as the driving force. Nonideal interface properties appear to limit the maximum attainable photovoltage to ~750 mV. Importantly, the a-Si:H photoelectrode can be durable when the proper solvent/electrolyte/redox couple combination is used. Sustained conversion (>100 h) of monochromatic 632.8-nm light (10 mW/cm^2) with an efficiency of ~3.3% has been demonstrated.

Acknowledgment. We thank the U.S. Department of Energy, Office of Basic Energy Sciences, Division of Chemical Sciences, and the Dow Chemical Company for support of the work at M.I.T. We thank Professor William Paul and Garrett Moddel of the Division of Applied Sciences, Harvard University, for useful discussions. M.S.L. acknowledges support from the Division of Applied Sciences, Harvard University, for graduate research performed at M.I.T.

Registry No. $Fe(Cp)_2$, 102-54-5; $Fe(Cp)_2^+$, 12125-80-3; [pentamethylferrocene]$^+$, 81064-27-9; pentamethylferrocene, 63074-30-6; [decamethylferrocene]$^+$, 54182-41-1; decamethylferrocene, 12126-50-0; MV^{2+}, 4685-14-7; MV^+, 25239-55-8; MV, 25128-26-1; $Ru(bpy)_3^{2+}$, 15158-62-0; $Ru(bpy)_3^+$, 56977-24-3; $Ru(bpy)_3$, 74391-32-5; $Ru(bpy)_3^-$, 56977-23-2; Pt, 7440-06-4; Si, 7440-21-3; (1,1′-ferrocenediyl)dichlorosilane, 66083-73-6; stainless steel, 12597-68-1.

Synthesis and X-ray Structure of *cis*-Tetracarbonyl[(*Z*)-(η^2-allylamino)(*p*-tolyl)carbene]-tungsten(0), a Stable Metal–Carbene–Alkene Complex

Charles P. Casey,* Alan J. Shusterman, Nicholas W. Vollendorf, and Kenneth J. Haller

Contribution from the Department of Chemistry, University of Wisconsin, Madison, Wisconsin 53706. *Received July 31, 1981*

Abstract: Allylamine and 1-amino-3-butene react with $(CO)_5WC(OCH_3)C_6H_4$-*p*-CH_3 to produce $(CO)_5WC(NHCH_2CH{=}CH_2)C_6H_4$-*p*-$CH_3$ ((*Z*)-**3** and (*E*)-**3**) and $(CO)_5WC(NHCH_2CH_2CH{=}CH_2)C_6H_4$-*p*-$CH_3$ ((*Z*)-**4** and (*E*)-**4**) as mixtures of isomers about the carbene carbon–nitrogen partial double bond. The alkene units in **3** and **4** are not coordinated to tungsten. Thermolysis or photolysis of a mixture of (*Z*)-**3** and (*E*)-**3** leads to formation of $(CO)_4\overline{WC(NHCH_2CH{=}CH_2)}C_6H_4$-*p*-$CH_3$ (**5**), a stable tungsten–carbene–alkene complex. The X-ray crystal structure of **5** shows a perpendicular arrangement of the alkene and carbene ligands. Crystal data for **5**: space group $P2_1/n$; $Z = 4$, $a = 7.989$ (1) Å, $b = 18.374$ (2) Å, $c = 10.875$ (1) Å, $\beta = 105.54$ (1)°; $V = 1538$ Å^3; $R = 0.037$ and $R_w = 0.047$ for the 2851 reflections with $F_o > 3\sigma(F_o)$. Attempts to prepare a tungsten–carbene–alkene complex with a larger chelate ring from **4** led to double-bond isomerization and isolation of $(CO)_4\overline{WC[NHCH_2CH{=}CHCH_3]}C_6H_4$-*p*-$CH_3$ (**11**).

Metal–alkene–carbene complexes and metallacyclobutanes have been proposed as key intermediates in several metal-catalyzed reactions. In the olefin metathesis reaction, the observed nonpairwise exchange of alkylidene groups is thought to occur via the equilibration of metal–alkene–carbene complexes and metallacyclobutanes.[1] The metal-catalyzed cyclopropanation of alkenes is proposed to occur by reductive elimination of the product cyclopropane from a metallacyclobutane intermediate.[2] In ad-

(1) Grubbs, R. H. *Prog. Inorg. Chem.* **1978**, *24*, 1–50. Katz, T. J. *Adv. Organomet. Chem.* **1977**, *16*, 283–317. Calderon, N.; Lawrence, J. P.; Ofstead, E. A. *Ibid.* **1979**, *17*, 449–492.

0002-7863/82/1504-2417$01.25/0

dition, an untested proposal for the heterogeneous Ziegler–Natta polymerization of alkenes involves cyclization of a metal–alkene–carbene complex as the carbon–carbon bond forming step.[3]

Only a few examples of stable metal–alkene–carbene complexes have been reported. In most cases, the alkene–metal bond is stabilized by chelation.[4-8] However, there are two examples of metal–alkene–carbene complexes in which the alkene (ethylene) is not attached to any other ligand.[9,10] Unfortunately, little information regarding the role of metal–alkene–carbene complexes in olefin metathesis and cyclopropanation has been dervied from studies of these complexes.

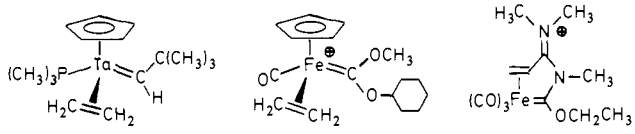

The only direct evidence for the conversion of a metal–alkene–carbene complex into a metallacyclobutane or a metallacyclobutane decomposition product is our recent discovery of a series of (alkenyloxy)carbene complexes of tungsten which decompose to cyclopropanes.[11] In the autocatalytic decomposition of $(CO)_5W[C(OCH_2CH_2CH{=}CH_2)C_6H_4\text{-}p\text{-}CH_3]$, **1**, two different tetracarbonyltungsten–alkene–carbene intermediates were detected by NMR and IR spectroscopy, both of which decomposed to cyclopropane **2**. The two carbene–alkene complexes are thought to differ in the relative orientations of the carbene and alkene ligands; the M=C and C=C bonds can be either parallel or perpendicular.

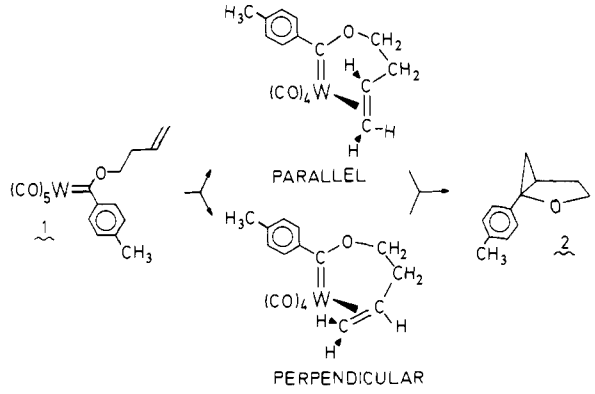

In an effort to prepare kinetically more stable tungsten–carbene–alkene complexes, we have studied related amino-substituted carbene complexes since the electron-donating nitrogen atom is well-known to stabilize metal–carbene complexes. Here we report the synthesis and X-ray crystal structure of the very stable tunsgten–carbene–alkene complex *cis*-tetracarbonyl[(*Z*)-(η^2-allylamino)(*p*-tolyl)carbene]tungsten(0), **5**.[11]

Results and Discussion

Synthesis of (Alkenylamino)carbene Complexes. Pentacarbonyltungsten–carbene complexes possessing an uncomplexed carbon–carbon double bond in a side chain were synthesized by reaction of methoxycarbene complexes with amino-substituted alkenes. Addition of allylamine to a red solution of $(CO)_5W{=}C(OCH_3)C_6H_4\text{-}p\text{-}CH_3$ in ether at room temperature led to an instantaneous formation of a yellow solution of pentacarbonyl[(allylamino)(*p*-tolyl)carbene]tungsten(0), **3**, which was isolated by preparative TLC as a moderately air-stable oil in 83% yield. The reaction of amines with methoxycarbene complexes occurs by nucleophilic attack of the amine at the electron-deficient carbene carbon atom followed by loss of methanol.[12] The ^1H and ^{13}C NMR spectra of this oil indicated the presence of a 1.2:1 mixture of two isomers, (*Z*)-**3** and (*E*)-**3**, which differed in the orientation of the allyl group about the carbene carbon–nitrogen partial double bond. Stereochemical assignment of the isomers was based on Fischer's observation[13,15] that the ^1H NMR resonances of alkyl groups cis to the metal (*Z* isomers) appear downfield from those trans to the metal (*E* isomers). The downfield NCH_2 resonance at δ 3.44 was assigned to isomer (*Z*)-**3** while the NCH_2 resonance at δ 2.84 was assigned to (*E*)-**3**.

Similarly, reaction of 1-amino-3-butene with $(CO)_5W{=}C(OCH_3)C_6H_4\text{-}p\text{-}CH_3$ gave an 87% yield of an isomeric mixture of pentacarbonyl[(3-butenylamino)(*p*-tolyl)carbene]tungsten(0) ([(*Z*)-**4**]:[(*E*)-**4**] = 1.9:1].

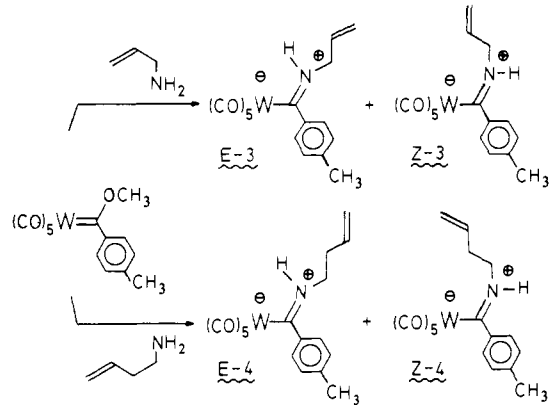

A Chelated (Allylamino)carbene]tungsten Complex. Thermolysis of the pentacarbonyl[(allylamino)carbene]tungsten complex, (*Z*)-**3** and (*E*)-**3**, leads to explusion of CO and formation of the chelated metal–carbene–alkene complex *cis*-tetracarbonyl[(*Z*)-(η^2-allylamino)(*p*-tolyl)carbene]tungsten(0), **5**. When a mixture of (*Z*)-**3** and (*E*)-**3** was heated at 90 °C in toluene for 19 h, metal–carbene–alkene complex **5** was formed and isolated as a yellow crystalline solid in 29% yield following silica gel chromatography.

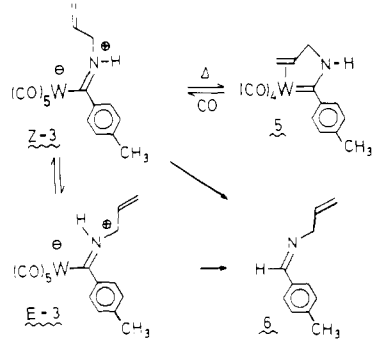

The structure of **5** was determined by both spectroscopy and X-ray diffraction (vide infra). As expected for a cis-disubstituted

(2) Nozaki, H.; Moriuti, S.; Takaya, H.; Noyori, R. *Tetrahedron Lett.* **1966**, 5239–5244. Nozaki, H.; Takaya, H.; Moriuti, S.; Noyori, R. *Tetrahedron* **1968**, *24*, 3655–3669. Moser, W. R. *J. Am. Chem. Soc.* **1969**, *91*, 1135–1140, 1141–1146.

(3) Ivin, K. J.; Rooney, J. J.; Stewart, C. D.; Green, M. L. H.; Mahtab, R. *J. Chem. Soc., Chem. Commun.* **1978**, 604–606.

(4) Mitsudo, T.; Nakanishi, H.; Inubushi, T.; Morishima, I.; Watanabe, Y.; Takegami, Y. *J. Chem. Soc., Chem. Commun.* **1976**, 416–417. Mitsudo, T.; Watanabe, Y.; Nakanishi, H.; Morishima, I.; Inubushi, T.; Takegami, Y. *J. Chem. Soc., Dalton Trans.* **1978**, 1298–1304. Nahatsu, K.; Mitsudo, T.; Nakanishi, H.; Watanabe, Y.; Takegami, Y. *Chem. Lett.* **1977**, 1447–1448.

(5) Nesmeyanov, A. N.; Sal'nikova, T. N.; Struchkov, Yu. T.; Andrianov, V. G.; Pogrebnyak, A. A.; Rybin, L. V.; Rybinskaya, M. I. *J. Organomet. Chem.* **1976**, *117*, C16–C20.

(6) Aumann, R.; Wörmann, H.; Kruger, C. *Angew. Chem., Int. Ed. Engl.* **1976**, *15*, 609–610.

(7) Hiraki, K.; Sugino, K.; Onishi, M. *Bull. Chem. Soc. Jpn.* **1980**, *53*, 1976–1981. Hiraki, K.; Sugino, K. *J. Organomet. Chem.* **1980**, *201*, 469–475.

(8) Dobrzyski, E. D.; Angelici, R. *J. Inorg. Chem.* **1975**, *14*, 1513–1518.

(9) Priester, W.; Rosenblum, M. *J. Chem. Soc., Chem. Commun.* **1978**, 26–27.

(10) Schultz, A. J.; Brown, R. K.; Williams, J. M.; Schrock, R. R. *J. Am. Chem. Soc.* **1981**, *103*, 169–176.

(11) A preliminary communication has appeared: Casey, C. P.; Shusterman, A. J. *J. Mol. Catal.* **1980**, *8*, 1–13. See also: Casey, C. P.; Shustermann, A. J.; Scheck, D. M. *Fundam. Res. Homogeneous Catal.* **1979**, *3*, 141–150.

(12) Fischer, E. O.; Heckl, B.; Kreiter, C. G. *J. Organomet. Chem.* **1971**, *28*, 367–389.

(13) Moser, E.; Fischer, E. O. *J. Organomet. Chem.* **1969**, *16*, 275–282.

Table I. Thermolysis of 3 at 80 °C[a,b]

time, h	(E)-3 enriched				(Z)-3 enriched			
	(Z)-3	(E)-3	5	6	(Z)-3	(E)-3	5	6
0	31	69	0	0	74	26	0	0
8.5	22	64	12		53	22	23	
19.0	13	60	18	5	30	22	38	10
36.0	5	54	22	12	21	20	41	14
83.2		32	26	24	11	10	41	26
135.5		27	25	26	5	7	41	29

[a] Thermolyses were carried out in C_6D_6 solvent in sealed NMR tubes and followed by 270-MHz ^1H NMR. [b] The percents given were determined by integration of the tolyl methyl peaks and comparison with the integration of the methyl peak of the internal standard *p*-bis(trimethylsilyl)benzene.

tetracarbonyltungsten complex,[14] **5** has intense IR bands at 2020 (s), 1934 (s), 1903 (s), and 1840 cm^{-1} (Nujol). The chelating alkene–carbene ligand of **5** makes the COs trans to one another nonequivalent; consequently, the ^{13}C NMR spectrum exhibits four carbonyl resonances at δ 204.3, 205.4, 210.9, and 214.9. In the ^1H NMR spectrum of **5**, coordination of the alkene moiety to tungsten shifts the ^1H NMR resonances of the vinyl protons 2–2.5 ppm upfield relative to those observed in (*Z*)-**3**, but the coupling constants of the vinyl hydrogens to one another in **5** are very similar to those observed for the uncomplexed alkene of (*Z*)-**3**. Similarly, in the ^{13}C NMR spectrum of **5**, coordination of the alkene shifts the resonances of the vinyl carbons 40–60 ppm upfield from those observed in (*Z*)-**3**. The chelate ring of **5** makes the NCH_2 protons chemically nonequivalent, and they appear in the ^1H NMR spectrum at δ 2.94 and 3.31.

The thermal production of **5** from **3** is accompanied by the formation of the allyl imine of *p*-tolualdehyde, **6**, and several other unidentified minor products. When **3** is heated under 600 psi of CO, formation of metal–carbene–alkene complex **5** is inhibited, and imine **6** becomes the major product (formed in >25% yield). The formation of aldehyde imines from $(CO)_5M{=}C(NHR)R'$ has been well documented. For example, $(CO)_5Cr{=}C(NHCH_3)C_6H_5$ produces the methyl imine of benzaldehyde in 90% yield after 72 h at 170 °C under 100 atm of CO.[15]

Several conclusions concerning the roles of (*E*)-**3** and (*Z*)-**3** in the formation of carbene–alkene complex **5** and of imine **6** arose from studies of the pyrolysis of enriched samples of (*E*)-**3** and of (*Z*)-**3** by ^1H NMR spectroscopy at 80 °C (Table I). First, the observation that different [(*Z*)-**3**]:[(*E*)-**3**] ratios are seen during their conversion to **5** and **6** requires that the equilibration of (*Z*)-**3** and (*E*)-**3** be slow relative to decomposition. Second, (*Z*)-**3** decomposes more rapidly than (*E*)-**3**, and its decomposition leads predominantly to carbene–alkene complex **5** (compare data at 19 h). The more rapid disappearance of (*Z*)-**3** causes the [(*Z*)-**3**]:[(*E*)-**3**] ratio to decrease with time. Third, imine **6** is apparently formed from both (*Z*)-**3** and (*E*)-**3**.[16] The tungsten–carbene–alkene complex **5** cannot be a major precursor of imine **6**, since thermal decomposition of **5** at 126 °C led to <5% **6** after 37 h. Fourth, some **5** apparently forms from (*E*)-**3** by a slow prior conversion to (*Z*)-**3**.[17] The formation of a 1:3.9 [(*E*)-**3**]:[(*Z*)-**3**] ratio when **5** was heated at 80 °C and 64 psi of CO also implies slow interconversion of (*Z*)-**3** and (*E*)-**3**. This slow interconversion is consistent with Fischer's observation that the barrier to rotation about the carbene carbon–nitrogen bond in $(CO)_5Cr{=}C[N(CH_3)_2]CH_3$ is greater than 25 kcal mol^{-1}.[18]

(14) Cotton, F. A. Inorg. *Chem.* **1964**, *3*, 702–711.
(15) Fischer, E. O.; Leupold, M. *Chem. Ber.* **1972**, *105*, 599–608.
(16) In the pyrolysis of the (*Z*)-**3**-enriched sample, the yield of imine **6** was always greater than the amount of (*E*)-**3** which had disappeared. For example, after 36 h at 80 °C, a 14% yield of imine **6** was observed but only 6% of the (*E*)-**3** initially present had disappeared. The remaining 8% yield of **6** is probably formed mainly from (*Z*)-**3**.
(17) For the (*E*)-**3**-enriched tube, the amount of **5** which formed was always close to the amount of (*Z*)-**3** which had disappeared. However, since some fraction of the (*Z*)-**3** which had disappeared at any time had been converted to **6**, some portion of **5** present had to be produced from (*E*)-**3**. Since **5** cannot be formed directly from (*E*)-**3**, these results indicate that (*E*)-**3** and (*Z*)-**3** are interconverted slowly at 80 °C.

Table II. Photolysis of 3 in C_6D_6[a,b]

time, h	(E)-3	(Z)-3	5
0.0	58	42	0
5.75	45	22	33
15.25	32	19	49
21.00	32	19	49

[a] Irradiation at 350 nm of 3 was carried out in a sealed NMR tube in C_6D_6 solvent. [b] These are relative amounts; other unidentified compounds were also observed in low yields (≤10% of 3 present at $t = 0$).

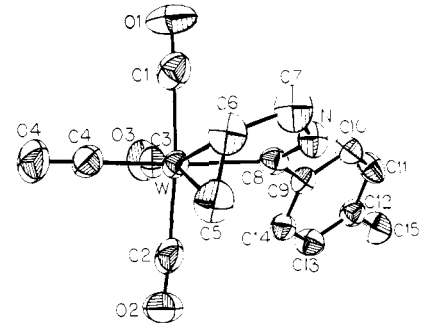

Figure 1. ORTEP drawing of **5** showing perpendicular arrangement of carbene and alkene ligands.

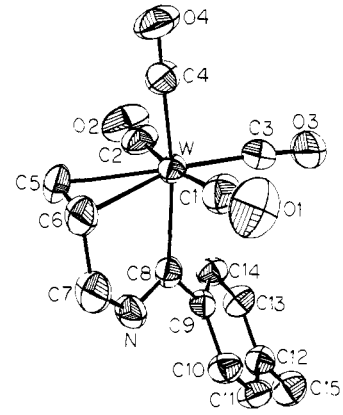

Figure 2. ORTEP drawing showing chelate ring of **5**.

Photolysis of **3** also leads to the formation of tungsten–carbene–alkene complex **5**. Irradiation of a benzene-d_6 solution of a 1.38:1 (*Z*)-**3**:(*E*)-**3** mixture at 350 nm (**3** has ε 9800 at 350 nm) was followed by NMR spectroscopy (Table II). As in the case of the thermal reaction, the disappearance of isomer (*Z*)-**3** was more rapid than that of (*E*)-**3**. However, the concentration of (*E*)-**3** dropped nearly half as fast as that of (*Z*)-**3**. The formation of tungsten–carbene–alkene complex **5** accounted for more than 90% of the amount of (*Z*)-**3** and (*E*)-**3** destroyed.

The photoisomerization of (*E*)-**3** to (*Z*)-**3** provides an attractive explanation of the photoconversion of (*E*)-**3** to **5**. This isomerization requires rotation about the carbene carbon–nitrogen partial double bond of **3**. While the photoisomerization of aminocarbene complexes has not been reported previously, it can readily be explained by referring to molecular orbital calculations on $(CO)_5CrC[N(CH_3)_2]C_6H_5$.[19] According to these calculations, the lowest excited state should arise from the promotion of an electron from the HOMO (a metal–CO π-bonding orbital centered primarily on the metal) to the LUMO (the π* orbital of the carbene carbon–metal bond which is centered on the carbene carbon). This π* orbital is π-antibonding between the nitrogen and the carbene carbon. Thus, isomerization of the amino group should occur readily in the excited state. Since the metal–CO bond is weakened by promotion of an electron out of the π metal–CO bonding

(18) Moser, E.; Fischer, E. O. *J. Organomet. Chem.* **1968**, *13*, 387–398.
(19) Block, T. F.; Fenske, R. F. *J. Organomet. Chem.* **1977**, *139*, 235–269.

Table III. Interatomic Distances (Å) and Angles (Deg) for 5[a]

		Distances			
W-C(1)	2.037 (10)	C(1)-O(1)	1.137 (10)	C(8)-C(9)	1.484 (8)
W-C(2)	2.029 (10)	C(2)-O(2)	1.150 (10)	C(9)-C(10)	1.392 (8)
W-C(3)	1.969 (8)	C(3)-O(3)	1.150 (10)	C(9)-C(14)	1.401 (9)
W-C(4)	1.980 (8)	C(4)-O(4)	1.167 (9)	C(10)-C(11)	1.378 (9)
W-C(5)	2.405 (7)	C(5)-C(6)	1.383 (13)	C(11)-C(12)	1.373 (10)
W-C(6)	2.414 (7)	C(6)-C(7)	1.492 (11)	C(12)-C(13)	1.391 (9)
W-C(8)	2.206 (7)	C(7)-N	1.459 (8)	C(13)-C(14)	1.388 (9)
		N-C(8)	1.292 (9)	C(12)-C(15)	1.497 (9)
		Angles			
C(1)-W-C(2)	171.9 (4)	C(3)-W-C(6)	160.8 (3)	C(7)-N-C(8)	122.7 (6)
C(1)-W-C(3)	86.6 (3)	C(3)-W-C(8)	95.6 (3)	N-C(8)-W	117.5 (5)
C(1)-W-C(4)	88.1 (3)	C(4)-W-C(5)	90.7 (3)	N-C(8)-C(9)	112.8 (6)
C(1)-W-C(5)	110.3 (3)	C(4)-W-C(6)	96.5 (3)	C(8)-C(9)-C(10)	121.8 (6)
C(1)-W-C(6)	77.6 (3)	C(4)-W-C(8)	170.1 (3)	C(8)-C(9)-C(14)	120.3 (5)
C(1)-W-C(8)	89.8 (3)	C(5)-W-C(6)	33.3 (3)	C(10)-C(9)-C(14)	117.9 (5)
C(2)-W-C(3)	86.1 (3)	C(5)-W-C(8)	81.0 (3)	C(9)-C(8)-W	130.1 (5)
C(2)-W-C(4)	89.0 (3)	C(6)-W-C(8)	73.6 (3)	C(9)-C(10)-C(11)	120.7 (6)
C(2)-W-C(5)	77.2 (3)	W-C(5)-C(6)	73.7 (4)	C(10)-C(11)-C(12)	122.1 (6)
C(2)-W-C(6)	110.1 (3)	W-C(6)-C(5)	72.9 (4)	C(11)-C(12)-C(15)	121.5 (6)
C(2)-W-C(8)	94.4 (3)	W-C(6)-C(7)	107.0 (4)	C(11)-C(12)-C(13)	117.6 (6)
C(3)-W-C(4)	93.9 (3)	C(5)-C(6)-C(7)	122.1 (8)	C(15)-C(12)-C(13)	120.8 (7)
C(3)-W-C(5)	162.6 (3)	C(6)-C(7)-N	111.4 (7)	C(12)-C(13)-C(14)	121.4 (6)
				C(13)-C(14)-C(9)	120.2 (6)

[a] The estimated standard deviations of the least significant digits are given in parentheses.

orbital, CO dissociation should also be facile in this excited state.

X-ray Crystal Structure of Tungsten–Carbene–Alkene Complex 5. An X-ray crystallographic study of **5** confirmed its structure as a tetracarbonyltungsten–carbene–alkene complex (Tables III and IV). Figure 1 illustrates the slightly distorted octahedral geometry of **5** and the approximately perpendicular arrangement of the carbene and alkene ligands. Figure 2 illustrates that the metallacycle including W, C(8), N, C(7), and C(6) is nearly planar.

There are three angles that fully define the relationship of a carbene and an alkene ligand in a metal complex. First, the angle α between the carbene carbon atom, the metal, and the midpoint of the alkene carbon–carbon double bond defines the gross relationship between the ligands. For a cis complex, $\alpha = 90°$, and for a trans complex, $\alpha = 180°$. Second, the angle β between the plane defined by the carbene carbon, the metal, and the midpoint of the alkene ligand and the plane defined by the metal and the two carbons of the alkene unit determines whether the carbon–carbon double bond of the alkene and the carbene carbon to metal bond are parallel ($\beta = 0°$) or perpendicular ($\beta = 90°$). Third, the angle γ defines the twist between the plane of the carbene carbon, the metal, and the alkene midpoint and the mean plane of the carbene ligand [M=C(R)R'].[20] For cis metal–carbene–alkene complexes ($\alpha = 90°$), four extreme geometries are possible, I–IV. Only conformation II ($\beta = 0°$, $\gamma = 90°$) is set up for a

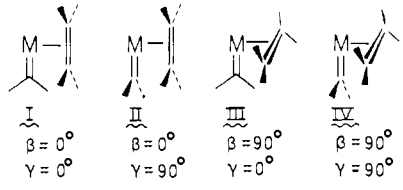

smooth conversion to a metallacyclobutane. For Schrock's tantalum–alkene–carbene complex,[10] $(C_5Me_5)Ta(CHCMe_3)(\eta^2\text{-}CH_2CH_2)(PMe_3)$, these angles are $\alpha = 110.6°$, $\beta = 86.6°$, and $\gamma = 1.0°$.

For **5**, the small size of the chelate ring between the carbene carbon and the complexed alkene pinches the two ligands together ($\alpha = 76.8°$). The carbene carbon is bent toward the alkene ligand, which reduces the angle between the carbene carbon, tungsten, and the CO trans to the carbene carbon ($\angle C(8)WC(4) = 170.1°$). Similarly, the angle between the midpoint of the alkene unit, tungsten, and the CO trans to the alkene is reduced ($\angle C(5)WC(3) = 172.4°$).

The carbene and alkene ligands are in a nearly perpendicular arrangement. The angle β between the plane defined by the carbene carbon, tungsten, and the midpoint of the alkene ligand and the plane of tungsten and the two alkene carbon atoms is 77.0°.

Table IV. Least-Squares Planes, Displacement from Mean Plane (Å), and Selected Angles between Planes (Deg)

	Plane 1		
W	−0.103	N	0.054
C(6)	0.182	C(8)	0.068
C(7)	−0.200		
	Plane 2		
W	0.0002	C(9)	0.0003
C(8)	−0.0009	N	0.0003
	Plane 3		
C(9)	0.015	C(12)	0.010
C(10)	0.002	C(13)	0.007
C(11)	−0.015	C(14)	−0.0019
	Plane 4		
W	0.032	C(4)	−0.015
C(3)	−0.003	C(8)	−0.014
	Plane 5		
W			
C(8)			
C(5)-C(6)[a]			
	Plane 6		
W			
C(5)			
C(6)			
	Plane 7		
W	−0.042	C(2)	0.022
C(1)	0.022	C(3)	−0.003
	Dihedral Angles		
planes 2 and 3	37.0	planes 5 and 6 (β)	103.0
planes 2 and 4	23.9	planes 6 and 7	13.8
planes 2 and 5 (γ)	25.7	planes 6 and 1	101.3

[a] The midpoint of the C(5)=C(6) bond of the alkene ligand.

(20) It should be noted that the relationship defined by β and γ are not affected by changes in α. For trans metal–alkene–carbene complexes ($\alpha = 180°$), β and γ are not defined, and the relationship of the ligands must be described in terms of δ, the angle between the plane of the metal and the two alkene carbons and the plane of the carbene ligand.

Before determining the crystal structure of **5**, we had made Dreiding models with parallel ($\beta = 0°, \gamma = 25°$) and perpendicular ($\beta = 90°, \gamma = 20°$) arrangements of the alkene and carbene ligands. Examination of the models indicated that either geometry was feasible but that some pinching together of the ligands would be required in either case. Similar examination of models having the appropriate bond lengths and angles fixed at the values observed in the crystal structure of **5** also indicated that both perpendicular and parallel conformations were sterically possible.

There are no obvious electronic factors that require the observed perpendicular conformation of **5**. Hoffmann and Eisenstein,[21] in discussing bonding in metal-carbene-alkene complexes, have suggested that the carbene and alkene ligands will preferentially π bond to different t_{2g} orbitals. This qualitative restriction can be fulfilled by either the parallel or perpendicular conformations available to the chelate system of **5**. Only geometries such as II are precluded, and such geometries are not possible for chelates joined by a small number of atoms as in the case of **5**. EHMO calculations on $CpTa(PH_3)(CH_2)(C_2H_4)$ indicate that perpendicular conformations are favored relative to parallel conformations. Unfortunately, the subject of the detailed calculations is drastically different from **5** both in the oxidation state of the metal and in the ligand environment; consequently, extensions to **5** are not warranted.

With no obvious steric or electronic factors that favor the observed perpendicular conformation of carbene and alkene ligands in **5**, it is not clear why the molecule exists in this conformation. For the (butenyloxy)carbene-alkene complex **1**, we observed two diffeent conformations (presumably the parallel and perpendicular). While we have no evidence for a parallel conformation of **5** in solution, such a conformation may not be much higher in energy than the observed perpendicular conformation.

The plane of the carbene ligand is twisted ($\gamma = 25.7°$) from the plane of the carbene carbon, tungsten, and the alkene midpoint. This twist is largely a result of constraints of the small chelate ring. The observed angle is smaller than the angle between the plane of the carbene ligand and the plane including two cis and one trans CO ligands in $(CO)_5CrC(OCH_3)C_6H_5$ (45°)[22] or $(CO)_5CrC(SC_6H_5)CH_3$ (36°)[23] but is comparable to that found for $(CO)_5WC(C_6H_5)_2$, **8** (18°).[24]

The alkene ligand of **5** is bonded symmetrically to tungsten with bond lengths that differ by less than 0.01 Å. The 1.38-Å carbon-carbon bond length of the alkene lignd in **5** is longer than the standard uncoordinated alkene bond length of 1.33 Å. However, it is substantially shorter than the 1.48-Å bond length of coordinated ethylene in $(C_5Me_5)Ta(CHCMe_3)(\eta^2\text{-}CH_2CH_2)(PMe_3)$; in this tantalum compound, there is much greater electron donation into the π^* level of ethylene, and the molecule has been described as a metallacyclopropane by Schrock. For the electronically more similar complex **7**, the bond length of the alkene bonded to molybdenum is 1.39 Å, which is similar to that observed for **5**.[25]

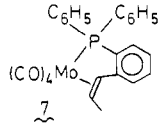

7

Attempted Synthesis of a (Butenylamino)carbene-Alkene-Tungsten Complex. While the (allylamino)carbene-alkene-tungsten complex **5** has an interesting structure, the compound does not lead to either cyclopropanes or olefin metathesis related alkene scission products upon thermolysis. This can be attributed to the reluctance to form a highly strained bicyclo[2.2.0] metallacycle which would be the precursor of either the bicyclo[2.1.0] system of the cyclopropane or the azacyclobutene ring of the alkene scission product. Similarly, in the case of the (allyloxy)carbene complex **9**, thermolysis failed to give either cyclopropane or alkene

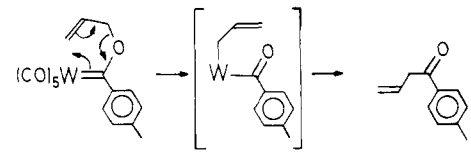

scission products. Instead, **9** thermally decomposes at 40 °C to slowly produce *p*-tolyl allyl ketone.[11] This reaction could proceed by electrocyclic rearrangement followed by reductive elimination.

Since the (butenyloxy)carbene complex **1** gave cyclopropane **2** upon thermal decomposition, we initiated a study of (butenylamino)carbene complexes in an effort to prepare an isolable metal-carbene-alkene complex that would also be a cyclopropane precursor. We have studied the thermal and photochemical reactions of the (butenylamino)carbene complex **4**, in which the alkene unit is not coordinated to tungsten. We were unable to detect any formation of the larger ring-chelated (butenylamino)carbene-alkene-tungsten complex **10**. Instead, isomerization of the alkene double bond occurred and we isolated complex **11**, which is a substituted (allylamino)carbene-alkene-tungsten complex similar to **5**.

Irradiation of DME solutions of **4** ([(*Z*)-**4**]:[(*E*)≥**4**] = 1.9:1) at either 254 or 360 nm resulted in a color change from yellow to orange, the appearance of new bands in the IR spectrum at 2010, 1975, and 1872 cm^{-1}, and the decrease in intensity of the band at 2058 cm^{-1} due to **4**. Preparative TLC lead to the isolation of a yellow band containing a 1:1.3 mixture of starting materials (*Z*)-**4** and (*E*)-**4** and a slower moving orange band containing the isomerized carbene-alkene-tungsten compound **11**.

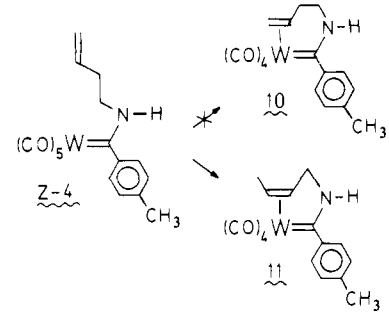

11 was characterized by IR and NMR spectroscopy. The resonances at δ 4.04 and 4.33 are assigned to the coordinated vinyl protons coupled to one another with a 9.3-Hz coupling constant characteristic of cis hydrogens on a carbon-carbon double bond.

The thermal reaction of **4** proceeds more slowly than that of the (allylamino)carbene complex **3** and leads to a complex mixture of products. Heating a solution of **4** ([(*Z*)-**4**]:[(*E*)-**4**] = 1.28:1) in C_6D_6 to 80 °C for 11 h led to little decomposition of **4** as shown by ^1H NMR spectroscopy. After being further heated at 80 °C for 32 h, the reaction mixture consisted of about 50% of the starting material ([(*Z*)-**4**]:[(*E*)-**4**] = 1:1), about 20% **11**, and several other unidentified products.

It is not known whether the double-bond isomerization involved in the conversion of **4** to **11** occurs before or after complexation of the alkene to tungsten. An analogous double-bond isomerization was observed by Bennett in the formation of **7**.[25]

Conclusion

Earlier we had found NMR evidence for a metastable tungsten-carbene-alkene complex formed from (butenyloxy)carbene complex **1** and showed that this complex was an intermediate in the formation of cyclopropane **2**. In this paper, we have exploited the stabilizing effect of amino groups on metal-carbene complexes to prepare the very stable tungsten-carbene-alkene complex **5** in which the carbene and alkene ligands have a nearly perpen-

(21) Hoffmann, R.; Eisenstein, O., private communication.
(22) Mills, O. S.; Redhouse, A. D. *J. Chem. Soc. A* **1968**, 642-647.
(23) Hoare, R. J.; Mills, O. S. *J. Chem. Soc., Dalton Trans.* **1972**, 653-656.
(24) Casey, C. P.; Burkhardt, T. J.; Bunnell, C. A.; Calabrese, J. C. *J. Am. Chem. Soc.* **1977**, *99*, 2127-2134.
(25) Interrante, L. V.; Bennett, M. A.; Nyholm, R. S. *Inorg. Chem.* **1966**, *5*, 2212-2217. Luth, H.; Truter, M. R.; Robson, A. *J. Chem. Soc. A* **1969**, 28-41.

dicular conformation. However, decomposition of **5** did not produce a cyclopropane, probably due to the instability of the required bicyclo[2.1.0] ring system. In continuing work, we are attempting to make stable metal–carbene–alkene complexes that can be isolated, structurally characterized, and then converted to either cyclopropanes or alkene scission products.

Experimental Section

General Procedures. ^1H NMR spectra were obtained on a Bruker WH-270 spectrometer; ^{13}C NMR spectra were obtained on JEOL FX-60 or FX-200 spectrometers. To minimize the effect of differences in relaxation times, a 30-s pulse repetition rate was employed for ^1H NMR spectra, when quantitative results were required. Infrared spectra were obtained on a Digilab FTS-20 interferometer or a Beckman IR-4230 spectrophotometer. Mass spectra were obtained on an AEI MS-902 mass spectrometer. UV–vis spectra were measured on a Cary 118 spectrophotometer. Melting points were determined on a Thomas-Hoover capillary melting point apparatus and are uncorrected. Photochemical experiments were carried out in a Rayonet Srinivasan–Griffin photochemical reactor. Low-pressure mercury lamps (maximum emission at 254 nm) and General Electric F8T5/BLB lamps (maximum emission at 350 nm) were used with the photochemical reactor. Constant-temperature thermolysis experiments were carried out in a thermostated silicone oil bath (±0.2 °C).

All reactions involving organometallic compounds were performed in flame-dried glassware under a nitrogen atmosphere. Diethyl ether and tetrahydrofuran (THF) were distilled from sodium and benzophenone under a nitrogen atmosphere. Dimethoxyethane (DME) was dried over $CaCl_2$ and then distilled from sodium and benzophenone on a vacuum line. Dichloromethane was distilled from P_2O_5 under a nitrogen atmosphere. Benzene-d_6 was distilled from sodium benzophenone and triglyme prior to its use in sealed-tube experiments. Toluene was dried over Linde 4A molecular sieves. Preparative thin-layer chromatography (TLC) was performed with Merck PF-254 silica gel.

Pentacarbonyl[(allylamino)(*p*-tolyl)carbene]tungsten(0) ((*Z*)-3 and (*E*)-3). When allylamine (0.75 mL, 10.0 mmol) was added to an ether solution of $(CO)_5WC(OCH_3)C_6H_4$-*p*-CH_3[26] (0.458 g, 1.0 mmol), the color of the solution immediately changed from red to yellow. Evaporation of solvent followed by preparative TLC (silica gel, 1:2 CH_2Cl_2–hexane) led to the isolation of a 1.2:1 mixture of (*Z*)-**3**:(*E*)-**3** (0.40 g, 83%) as a yellow oil; IR (CH_2Cl_2) 2064 (m), 1970 (w), 1928 (vs) cm^{-1}.

NMR spectra of two different mixtures of (*Z*)-**3** and (*E*)-**3** were obtained and peaks were assigned to the major and minor isomers on the basis of the relative intensities. See Results for stereochemical assignments of isomers.

For (*Z*)-**3**: ^1H NMR (270 MHz, C_6D_6) δ 2.02 (s, 3 H), 3.94 (tm, *J* = 5.7 Hz, 2 H), 4.79 (dm, *J* = 17.0 Hz, 1 H), 4.87 (dm, *J* = 10.3 Hz, 1 H), 5.34 (ddt, *J* = 17.1, 10.3, 5.7 Hz, 1 H), 6.67 (d, *J* = 8.1 Hz, 2 H), 6.83 (d, *J* = 7.5 Hz, 2 H), 7.27 (br s, 1 H); $\{^1H\}^{13}C$ NMR (50 MHz, CD_3CN, 0.07 M $Cr(acac)_3$) δ 21.1 (CH_3), 58.3 (NCH_2), 118.9 (CH=*C*H_2), 123.3, 129.4 (ortho, meta), 132.9, 138.7, 153.0 (ipso, para, *C*H=CH_2), 199.0 (cis CO, $J_{^{183}W-^{13}C}$ = 126 Hz), 204.8 (trans CO, $J_{^{183}W-^{13}C}$ = 126 Hz), 255.7 (carbene).

For (*E*)-**3**: ^1H NMR (270 MHz, C_6D_6) δ 1.98 (s, 3 H), 2.84 (tm, *J* = 5.7 Hz, 2 H), 4.68 (dm, *J* = 9.0 Hz, 1 H), 4.70 (dm, *J* = 18.2 Hz, 1 H), 4.91 (ddt, *J* = 16.5, 10.7, 5.1 Hz, 1 H), 6.52 (d, *J* = 8.1 Hz, 2 H), 6.83 (d, *J* = 7.5 Hz, 2 H), 8.29 (br s, 1 H); $\{^1H\}^{13}C$ NMR (50 MHz, CD_3CN, 0.07 M $Cr(acac)_3$) δ 21.1 (CH_3), 52.7 (NCH_2), 118.3 (CH=*C*H_2), 120.6, 129.4 (ortho, meta), 133.0, 137.3, 148.2 (*C*H=CH_2, ipso, para), 199.3 (cis CO, $J_{^{183}W-^{13}C}$ = 126 Hz), 205.1 (trans CO, $J_{^{183}W-^{13}C}$ = 126 Hz), 257.2 (carbene).

Pentacarbonyl[(3-butenylamino)(*p*-tolyl)carbene]tungsten(0) ((*Z*)-4 and (*E*)-4). Addition of 1-amino-3-butene[27] (100 mg, 1.41 mmol) to an ether solution of $(CO)_5WC(OCH_3)C_6H_4$-*p*-CH_3 followed by evaporation of solvent and preparative TLC (silica gel, 2:1 hexane–CH_2Cl_2) gave a 1.9:1 mixture of (*Z*)-**4**:(*E*)-**4** (94 mg, 87%) as a yellow oil; IR (hexane) 2065 (m), 1973 (w), 1940 (s), 1930 (sh), 1918 (sh) cm^{-1}. NMR spectra of the major and minor isomers were assigned on the basis of relative intensities.

For (*Z*)-**4**: ^1H NMR (270 MHz, C_6D_6) δ 1.90 (q, *J* = 6.5 Hz, 2 H), 2.07 (s, 3 H), 3.52 (q, *J* = 6.1 Hz, 2 H, NCH_2), 4.9 (m, 2 H), 5.45 (m, 1 H), 6.79 (d, *J* = 6.8 Hz, 2 H), 6.91 (d, *J* = 7.0 Hz, 2 H), 7.70 (br s, 1 H); ^{13}C NMR (50 MHz, gated decoupled, CD_3CN, 0.07 M $Cr(acac)_3$) δ 21.0 (q, *J* = 127 Hz, CH_3), 33.6 (t, *J* = 127 Hz, NCH_2CH_2), 55.4 (t, *J* = 137 Hz, NCH_2), 123.2 (d, *J* = 161 Hz, ortho or meta), 129.3 (d, *J* = 159 Hz, ortho or meta), 134.9 (d, *J* = 152 Hz, *C*H=CH_2), 138.6, 153.0 (s, s, ipso and para), 199.1 ($J_{^{183}W-^{13}C}$ = 126 Hz, cis CO), 204.7 (trans CO), 254.1 (carbene), not observed (CH=*C*H_2).

For (*E*)-**4**: ^1H NMR (270 MHz, C_6D_6) δ 1.55 (q, *J* = 6.4 Hz, 2 H), 2.06 (s, 3 H), 2.47 (q, *J* = 6.0 Hz, 2 H, NCH_2), 4.9 (m, 2 H), 5.18 (m, 1 H), 6.57 (d, *J* = 6.6 Hz, 2 H), 6.91 (d, *J* = 7.0 Hz, 2 H), 8.48 (br s, 1 H); ^{13}C NMR (50 MHz, gated decoupled, CD_3CN, 0.07 M $Cr(acac)_3$) δ 21.0 (q, *J* = 127 Hz, CH_3), 49.8 (t, *J* = 145 Hz, NCH_2CH_2), 66.0 (t, *J* = 132 Hz, NCH_2), 120.8 (d, *J* = 162 Hz, ortho or meta), 129.3 (d, *J* = 159 Hz, ortho or meta), 137.1, 148.4 (s, s, ipso and para), 199.3 (cis CO, $J_{^{183}W-^{13}C}$ = 126 Hz), 205.1 (trans CO), 255.9 (carbene), not observed (*C*H=CH_2 and CH=*C*H_2).

***cis*-Tetracarbonyl[(*Z*)-(η²-allylamino)(*p*-tolyl)carbene]tungsten(0) (5).** A mixture of (*Z*)-**3** and (*E*)-**3**, prepared by reaction of allylamine (23.3 mmol) with $(CO)_5WC(OCH_3)C_6H_4$-*p*-CH_3 (3.56 g, 7.77 mmol) and purified by passage through a short silica gel column, was dissolved in toluene, degassed by three freeze–pump–thaw cycles, and heated to 90 °C for 19 h. Solvent was evaporated and the residue was subjected to column chromatography on silica gel. Development with 1:2 CH_2Cl_2–hexane led to the elution of a yellow band consisting of a 1:4.6 mixture of (*Z*)-**3**:(*E*)-**3** (36% yield) followed by an orange band. Evaporation of solvent from the orange solution gave **5** as a yellow solid: mp 145–146.5 °C; IR (Nujol) 2020 (s), 1934 (s), 1903 (s), 1840 (s) cm^{-1}; ^1H NMR (270 MHz, C_6D_6) δ 2.00 (s, 3 H), 2.81 (d, *J* = 13.2 Hz, 1 H, C=C*H*H), 2.94 (br d, *J* = 14.1 Hz, 1 H, diastereotopic NCH_2), 3.06 (d, *J* = 8.6 Hz, 1 H, C=CH*H*), 3.31 (ddd, *J* = 14.1, 5.1, 1.6 Hz, 1 H, diastereotopic NCH_2), 4.09 (ddddd, *J* = 13.1, 8.8, 4.8, 4.0, 0.7 Hz, 1 H, *C*H=CH_2), 6.82 (d, *J* = 8.0 Hz, 2 H), 6.92 (d, *J* = 8.0 Hz, 2 H), 7.26 (br s, 1 H, NH). Decoupling of the secondary vinylic hydrogen by irradiation at δ 4.09 results in collapse of the terminal vinyl hydrogen resonances at δ 2.81 and 3.06 to singlets and to simplification of the NCH_2 resonance to a doublet at δ 3.31 (J_{gem} = 14.3 Hz) and doublet of doublets at δ 2.94 (J_{gem} = 14.3 Hz, J_{NH} = 4.1 Hz). $\{^1H\}^{13}C$ NMR (15 MHz, CD_3CN, 0.07 M $Cr(acac)_3$) δ 21.3 (CH_3), 53.4, 61.7, 77.1 (CH_2=CHCH_2), 126.9, 129.9 (ortho, meta), 141.7, 145.9 (ipso, para), 204.3, 205.4, 210.9, 214.9 (COs), 258.1 (carbene). MS calcd for $C_{15}H_{13}NO_4{}^{184}W$, 455.0355; found, 455.0337.

In the thermal and photochemical reactions of (*Z*)-**3** and (*E*)-**3**, the allyl imine of *p*-tolualdehyde, **6**, was encountered as a side product that was identified in solution by spectral comparison with an authentic sample. The imine was prepared from allylamine (0.26 g, 4.55 mmol) and *p*-tolualdehyde (0.5 g, 4.16 mmol) in 10 mL of benzene by azeotropic distillation of water. Vacuum distillation of the reaction mixture gave **6** (0.6 g, 83%): IR (neat) 1650 (s), 1642 (m) cm^{-1}; ^1H NMR (270 MHz, C_6D_6) δ 2.04 (s, 3 H), 4.08 (dm, *J* = 5.5 Hz, 2 H), 5.07 (dm, *J* = 10.5 Hz, 1 H), 5.25 (dm, *J* = 17.3 Hz, 1 H), 6.06 (ddt, *J* = 16.4, 10.6, 5.5 Hz, 1 H), 6.96 (d, *J* = 7.9 Hz, 2 H), 7.70 (d, *J* = 7.9 Hz, 2 H), 7.97 (s, 1 H).

Crystallographic and X-ray Data. Crystals of **5** suitable for X-ray diffraction studies were obtained by vapor diffusion of hexane into a diethyl ether solution of **5**. A single crystal of approximate dimensions 0.5 × 0.6 × 0.6 mm was mounted on a glass fiber and coated with epoxy cement to prevent contact with the atmosphere. Preliminary examination of the crystal on a Syntex P$\bar{1}$ diffractometer showed the crystal to be monoclinic. The systematic absences of *h*0*l* when *h* + *l* = 2*n* + 1 and 0*k*0 when *k* = 2*n* + 1 are unique for the space group $P2_1/n$ (No. 14).[28] The unit cell parameters (at 19 ± 1 °C; λ (Mo Kα) = 0.710 73 Å) are *a* = 7.989 (1) Å, *b* = 18.374 (2) Å, *c* = 10.875 (1) Å, and β = 105.54 (1)°. These parameters were determined from a least-squares refinement utilizing the setting angles of 38 accurately centered reflections (35° < 2θ < 43°), each collected at ±2θ. The unit cell volume of 1538 Å^3 led to a calculated density of 1.96 g/cm^3 for 4 formula units of $WO_4NC_{15}H_{13}$ per unit cell. Repeated density measurements of crystals of **5** by flotation methods gave a value of 1.88 g/cm^3. We cannot explain the lower value of the observed density.

X-ray intensity data were collected with a Syntex P$\bar{1}$ diffractometer equipped with a graphite-monochromated Mo Kα radiation source. A total of 3505 unique refletions with $(\sin\theta)/\lambda \leq 0.649$ Å^{-1} were collected by using a θ–2θ step-scan technique with a scan range of 0.8° below 2θ(Mo $K\alpha_1$) to 0.8° above 2θ(Mo $K\alpha_2$) and a variable scan rate (2.0–24.0°/min). Throughout data collection, four standard reflections from diverse regions of reciprocal space were monitored every 50 reflections. The intensities of the standard reflections showed no systematic variations during the time required to collect the data. The intensity data were reduced and standard deviations calculated by methods similar to those described previously.[29] Absorption corrections were applied (empirical

(26) Bodner, G. M.; Kahl, S. B.; Bork, K.; Storhoff, B. N.; Wuller, J. E.; Todd, L. J. *Inorg. Chem.* **1973**, *12*, 1071–1074.

(27) 1-Amino-3-butene was prepared by the $LiAlH_4/AlCl_3$ reduction of allyl cyanide. Nystrom, R. F. *J. Am. Chem. Soc.* **1955**, *77*, 2544–2545.

(28) "International Tables for X-Ray Crystallography"; Kynoch Press: Birmingham, England, 1965; Vol. 1, p 99.

Table V. Fractional Monoclinic Coordinates for 5[a]

atom	x	y	z
W	0.21208 (3)	0.16047 (1)	0.49677 (2)
C(1)	0.2059 (11)	0.2699 (5)	0.5250 (7)
O(1)	0.2080 (13)	0.3311 (3)	0.5413 (8)
C(2)	0.2551 (12)	0.0528 (5)	0.4764 (7)
O(2)	0.2874 (11)	−0.0074 (4)	0.4655 (7)
C(3)	0.4412 (11)	0.1615 (4)	0.6223 (7)
O(3)	0.5711 (8)	0.1621 (3)	0.7000 (6)
C(4)	0.3080 (11)	0.1807 (4)	0.3502 (7)
O(4)	0.3669 (10)	0.1914 (4)	0.2646 (5)
C(5)	−0.0572 (11)	0.1203 (5)	0.3545 (7)
C(6)	−0.0855 (10)	0.1906 (5)	0.3899 (7)
C(7)	−0.1749 (10)	0.2062 (6)	0.4912 (6)
N	−0.0977 (8)	0.1651 (3)	0.6073 (5)
C(8)	0.0620 (9)	0.1434 (3)	0.6376 (6)
C(9)	0.1146 (7)	0.1097 (3)	0.7663 (5)
C(10)	0.0562 (9)	0.1364 (4)	0.8673 (6)
C(11)	0.1078 (9)	0.1045 (4)	0.9861 (6)
C(12)	0.2146 (9)	0.0446 (4)	1.0096 (6)
C(15)	0.2700 (12)	0.0106 (5)	1.1393 (7)
C(13)	0.2752 (10)	0.0181 (4)	0.9097 (6)
C(14)	0.2297 (9)	0.0507 (4)	0.7903 (6)

[a] The estimated standard deviations of the least significant digits are given in parentheses.

ψ scan method, $\mu_{Mo} = 7.24$ mm^{-1}). The minimum and maximum multipliers were 1.00 and 1.54, respectively.

The structure was solved by the heavy-atom method and refined by full-matrix least-squares techniques (the 2851 reflections with $F_o > 3\sigma(F_o)$ were used). A Patterson map revealed the position of the tungsten atom and a difference electron density map revealed the other nonhydrogen atoms. Atomic form factors for the nonhydrogen atoms were taken from Cromer and Waber[30] and that for hydrogen was taken from Stewart, Davidson, and Simpson.[31] The effects of anomalous scattering of the tungsten atom were included in the calculated structure amplitudes.[32] After refinement on the isotropic model converged, hydrogen atoms were included in the model in idealized positions as fixed contributors, each with an isotropic thermal parameter 1 Å^2 larger than the thermal parameter of the atom to which the hydrogen atom is attached. The nonhydrogen atoms were assumed to vibrate anisotropically, and the model was refined to convergence. At convergence the discrepancy indices were $R_1 = \sum||F_o| - |F_c||/\sum|F_o| = 0.037$ and $R_2 = \sum w(F_o - F_c)^2/[\sum w(F_o^2)]^{1/2} = 0.047$. The estimated standard deviation of an observation of unit weight was 1.69, and the final data/parameter ratio was 15.0. The highest peak on the final difference electron density map was about 14% of the height of a typical carbon atom peak. Atomic coordinates for the nonhydrogen atoms are given in Table V. Selected interatomic distances and angles are given in Table III. The anisotropic thermal parameters for the nonhydrogen atoms and the fixed parameters for the hydrogen atoms are given in Tables VI and VII in the supplementary material. Root-mean-square amplitudes of vibration (Table VIII) and a listing of final observed and calculated structure factor amplitudes (Table IX) are available as supplementary material.

***cis*-Tetracarbonyl[(*Z*)-(η^2-*cis*-2-butenylamino)(*p*-tolyl)carbene]tungsten(0) (11).** A solution of **4** (196 mg, 0.418 mmol, [(*Z*)-**4**]:[(*E*)-**4**] = 2.0:1) in 19 mL of DME in a Vycor tube sealed under vacuum was irradiated at 350 nm for 100 h. Preparative TLC (silica gel, 2:1 hexane–CH_2Cl_2) gave three colored bands. The fastest moving yellow band (R_f 0.41) contained **4** (107.4 mg, 55% recovery, [(*Z*)-**4**]:[(*E*)-**4**] = 1:1.7). The second yellow band (R_f 0.22, 59.2 mg) was a complex mixture of unidentified compounds. The slowest moving orange band consisted of an orange oil spectrally identified as **11** (42.0 mg, 23% yield, R_f 0.13).

For **11**: ^{1}H NMR (270 MHz, C_6D_6) δ 1.80 (dd, J = 6.4, 0.7 Hz, 3 H), 2.00 (s, 3 H), 3.01 (ddm, J = 14.2, 5.3 Hz, 1 H, diastereotopic NCH_2), 3.20 (ddd, J = 14.3, 5.8, 1.8 Hz, 1 H, diastereotopic NCH_2), 4.04 (dq, J = 9.3, 6.5 Hz, 1 H, C=C*H*CH$_3$), 4.33 (dt, J = 9.7, 5.0 Hz, 1 H, CH$_2$C*H*=C), 6.81 (d, J = 7.9 Hz, 2 H), 6.93 (d, J = 7.9 Hz, 2 H); IR (DME) ν(CO) 2010 (m), 1911 (s), 1892 (m), 1871 (m); IR (hexane) ν(CO) 2020 (s), 1930 (s), 1908 (s), 1898 (s) cm^{-1}.

Acknowledgment. Support from the National Science Foundation is gratefully acknowledged.

Registry No. (*Z*)-**3**, 77310-68-0; (*E*)-**3**, 77397-82-1; (*Z*)-**4**, 80975-95-7; (*E*)-**4**, 81025-23-2; **5**, 80975-96-8; **6**, 80975-83-3; **11**, 80975-94-6; (CO)$_5$WC(OCH$_3$)C$_6$H$_4$-*p*-CH$_3$, 38669-72-6.

Supplementary Material Available: Tables VI–IX (16 pages). Ordering information is given on any current masthead page.

(29) Whitesides, T. H.; Slaven, R. W.; Calabrese, J. C. *Inorg. Chem.* **1974**, *13*, 1895–1899.
(30) Cromer, D. T.; Waber, J. T. "International Tables for X-Ray Crystallography"; Kynoch Press: Birmingham, England, 1974; Vol. 4, pp 99–101, Table 2.2B.
(31) Stewart, R. F.; Davidson, E. R.; Simpson, W. T. *J. Chem. Phys.* **1965**, *42*, 3175–3187.
(32) Cromer, D. T.; Liberman, D. *J. Chem. Phys.* **1970**, *53*, 1891–1898.